Geosci. Model Dev. Discuss., https://doi.org/10.5194/gmd-2019-92
Manuscript under review for journal Geosci. Model Dev.
Discussion started: 2 May 2019

Geoscientific Model Development Discussions

Improving the LPJmL4-SPITFIRE vegetation-fire model for South America using satellite data

Markus Drüke[1,2], Matthias Forkel[3], Werner von Bloh[1], Boris Sakschewski[1], Manoel Cardoso[4], Mercedes Bustamante[5], Jürgen Kurths[1,2], and Kirsten Thonicke[1]

[1]Potsdam Institudte for Climate Impact Research, Telegraphenberg A 31, Potsdam, Germany
[2]Humboldt Universität zu Berlin, Unter den Linden 6, 10099 Berlin, Deutschland
[3] TU Wien, Department of Geodesy and Geoinformation, Gusshausstr. 27-29, 1040 Vienna, Austria
[4]Instituto Nacional de Pesquisas Espaciais, Av. dos Astronautas, 1.758 - Jardim da Granja, São José dos Campos - SP, 12227-010, Brazil
[5]Instituto de Ciências Biologicas, Universidade de Brasília, Campus Universitário Darcy Ribeiro - Asa Norte, 70910-900 Brasília, Brazil

Correspondence: Markus Drüke (drueke@pik-potsdam.de)

Abstract. Vegetation fires influence global vegetation distribution, ecosystem functioning, and global carbon cycling. Specifically in South America, changes in fire occurrence together with land use change accelerate ecosystem fragmentation and increase the vulnerability of tropical forests and savannas to climate change. Dynamic Global Vegetation Models (DGVMs) are valuable tools to estimate the effects of fire on ecosystem functioning and carbon cycling under future climate changes. However, fire-enabled DGVMs have partly poor performances in capturing the magnitude, spatial patterns, and temporal dynamics of burnt area as observed by satellites. As fire is controlled by the interplay of weather conditions, vegetation properties and human activities, fire modules in DGVMs can be improved in various aspects. As a starting point, we here focus on improving the controls of climate and hence fuel moisture content on fire danger in the LPJmL4-SPITFIRE DGVM in South America and especially for the Brazilian fire-prone biomes Caatinga and Cerrado. We therefore test two alternative model formulations (standard Nesterov index and a newly implemented water vapor pressure deficit) for climate effects on fire danger within a formal model-data integration setup where we estimate model parameters against satellite data sets of burnt area (GFED4) and above ground biomass of trees. Our results show that the optimized model improves the representation of spatial patterns and the seasonal to inter-annual dynamics of burnt area especially in the Cerrado/Caatinga region. In addition, the model improves the simulation of above-ground biomass and plant functional types (PFTs). We obtained the best results by using the water vapor pressure deficit (VPD) for the calculation of fire danger. The VPD includes, in comparison to the Nesterov index, a representation of the air humidity and the vegetation density. This work shows the successful application of a systematic model-data integration setup, as well as the integration of a new fire danger formulation, in order to optimize a process-based fire-enabled DGVM. It further highlights the potential of this approach to achieve a new level of accuracy in comprehensive global fire modelling and prediction.

Geosci. Model Dev. Discuss., https://doi.org/10.5194/gmd-2019-92
Manuscript under review for journal Geosci. Model Dev.
Discussion started: 2 May 2019

Geoscientific Model Development Discussions

1 Introduction

Fire in the Earth system is an important disturbance leading to many changes in the vegetation and has substantial impact on biodiversity, human health and ecosystems (Langmann et al., 2009). Fire is responsible for ca. 2 Pg of carbon emissions, which constitutes 20 % of global carbon emissions (Giglio et al., 2013; Werf et al., 2010). Fire-induced aerosol emissions and land surface changes modify evapotranspiration and surface albedo and have therefore a crucial impact on global climate (van der Werf et al., 2008; Yue and Unger, 2018). Despite of a recent decline in global burnt area (Andela et al., 2017), more frequent and intense drought-periods lead worldwide to increasing fire-prone weather and surface conditions therefore fire danger (Jolly et al., 2015). Growing fire danger along with land-use change are increasing ecosystem's vulnerability, which can in turn shift entire regions into a less vegetated state (Silvério et al., 2013). To account for these effects, it is extremely important to include well performing fire modules in Dynamic Global Vegetation Models (DGVMs).

Especially in South America, tropical forests, woodlands and other ecosystems are vulnerable to increasing fire danger and land use change. This paper focuses on the fire behaviour in central-northern South America and especially on the Brazilian fire-prone biomes Caatinga and Cerrado (Fig. 1). Together with the Amazon rainforest they form an area of very high biodiversity and have a large impact on the global carbon-cycle and the regional water cycle (Lahsen et al., 2016). Compared

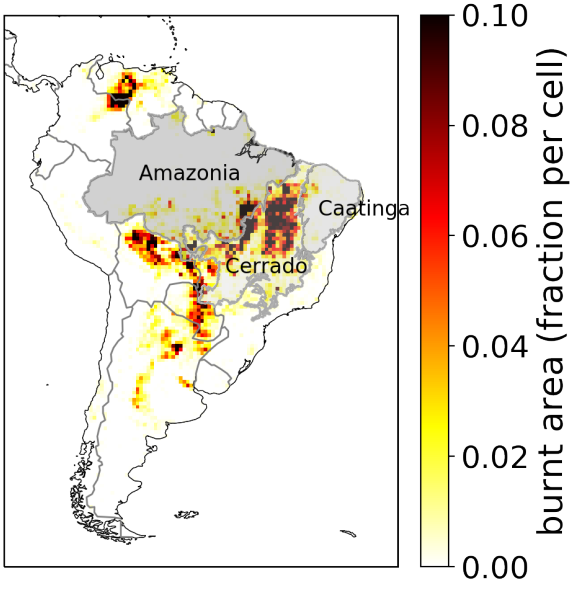

Figure 1. Overview of the mean annual burnt area in Brazil from 2005-2015 (Werf et al., 2017; Giglio et al., 2013) and the biomes Amazonia, Cerrado and Caatinga (IBGE, 2019; Harvard, 2019)

to the Amazon, the Cerrado and Caatinga are less densely vegetated and drier biomes, but with very different vegetation and precipitation dynamics. The Cerrado is a savanna-like biome with a mixture of shrubs, high grasses and dry forest parts. With a precipitation of ca. 1500 mm per year the Cerrado does experience a rainy season. The Caatinga, on the other hand, has

Geosci. Model Dev. Discuss., https://doi.org/10.5194/gmd-2019-92
Manuscript under review for journal Geosci. Model Dev.
Discussion started: 2 May 2019

a semi-arid climate with irregular rainfall between 500 and 750 mm per year, mostly within only a few months of the year. The vegetation is heterogeneous and characterized by deciduous dry forest and shrubs (Alvares et al., 2013; Prado, 2003). The different vegetation types lead to different fire spread, fire intensity, fire resistance and fire mortality properties. While within the Cerrado fire is a frequent event and the plants are mostly adapted to it (70 % of burnt area in Brazil is within the Cerrado, Moreira de Araújo et al., 2012), the Caatinga has a lower fire intensity and fire spread due to a lower biomass, which is available for fuel. Such variability in the vegetation and dead fuel composition, within and between biomes, poses a challenge to global fire models to correctly simulate observed fire patterns for a variety of biomes. Both, the Caatinga and the Cerrado depend on a strict equilibrium of fire-vegetation-climate feedbacks (Lasslop et al., 2016), which is threatened to be disturbed by human impact through climate change and land use change (Beuchle et al., 2015). While the Amazon is the focus of various national and international conservation efforts and at least by law well protected, the Cerrado is currently over-exploited by the agribusiness and its importance for regional climate, biodiversity and the water cycle is often neglected (Lahsen et al., 2016). In particular the disturbance of increasing fire regimes by climate change and land-use change might accelerate biome degradation. These effects on the Cerrado might also impact the Amazon rainforest by shifting the position of the savanna-forest biome boundary towards forest, putting the functioning of the Amazon rain forest at risk (Chambers and Artaxo, 2017). Parts of the Cerrado are also itself vulnerable to increasing fire regimes, and might shift to a less vegetated state, similar to the Caatinga (Hoffmann et al., 2000). To model these feedback-processes and to study the range of biome-stability under certain drought-induced perturbations, a realistic fire representation in climate and vegetation models is essential. However the modelling of the fire behaviour of the Brazilian Cerrado and Caatinga presents a huge challenge.

The fire occurrence depends on many interconnected parameters as humidity, precipitation, temperature, ignition sources (lightning and human) and windspeed, but also on fuel load, fuel moisture and the adaption of plant traits to fire (Keeley et al., 2011), which makes the development of fire models a complex task (Forkel et al., 2019; Hantson et al., 2016; Lasslop et al., 2015; Krawchuk and Moritz, 2011; Jolly et al., 2015). Global fire modelling is done either by empirical models (e.g. Thonicke et al., 2001; Knorr et al., 2016; Forkel et al., 2017) or by process-based models (e.g. Venevsky et al., 2002; Thonicke et al., 2010). Empirical fire models are simplified statistical representations of fire processes and are based on empirical relationships between variables (e.g. soil moisture and fire occurrence). Process-based fire models attempt to simulate fire via explicit process-based relations: Fire ignitions are calculated by taking into account lightning flashes as natural sources and human ignitions. The chance of an ignition to become a spreading fire is then determined by the fire danger index. Sophisticated fire models have further a function for calculating the rate of spread by taking into account wind speed and then translate these results into an area burnt, fuel consumption and fire carbon emissions (Thonicke et al., 2010; Hantson et al., 2016).

Weather conditions control the moisture content of fuels and the danger of fire ignitions and spread. Hence the simulation of fire danger plays an important role to simulate the occurrence of fire within global process-based fire models (Pechony and Shindell, 2009). Temperature, precipitation, humidity and vegetation-related variables are often used to compute fire weather indices and hence to estimate the risk of fire ignitions or spread (Chuvieco et al., 2010). Various fire weather indices have been previously developed and are used within operational fire danger assessment systems (e.g. Canadian Fire Weather index (FWI) (Wagner et al., 1987), the Keetch Byram Drought Index (Keetch and Byram, 1968), the Angström Fire Danger Index (Arpaci

et al., 2013), and the Nesterov index (Venevsky et al., 2002)). However, regional studies show that fire weather indices have different predictive performances for fire occurrence (Arpaci et al., 2013). Hence, the performance of different fire weather indices should be ideally assessed in order to accurately represent fire danger in DGVMs. However, not all fire weather indices can be easily adapted for global fire models because they require input variables that are not available within a DGVM framework. Hence a fire danger index for a DGVM should be as complex as necessary but still relatively easy to implement. As a result, the relatively simple Nesterov index has been widely used within global fire models (Venevsky et al., 2002; Thonicke et al., 2010).

Here, we aim to improve the simulated occurrence of fire (i.e. burnt area) in the LPJmL4-SPITFIRE model for South America and in particular for the fire-prone biomes Cerrado and Caatinga. We aim to test the performance of two alternative fire danger indices within SPITFIRE (based on the already implemented Nesterov index (Venevsky et al., 2002) and the newly implemented water vapour pressure deficit (Pechony and Shindell, 2009; Ray et al., 2005). Furthermore, we apply a formal model-data integration framework (LPJmLmdi, Forkel et al., 2014) to estimate model parameters that control fire danger, fire behaviour fire resistance and mortality against satellite-based data sets of burnt area and above-ground biomass (Fig. 2). Our approach is likely to improve the representation of spatial-temporal variations in fire behaviour in different climates and biomes to enable a much better modelling of the impact of climate change on fire-vegetation interactions in the current century.

2 Materials and Methods

2.1 The coupled vegetation-fire model LPJmL4-SPITFIRE

2.1.1 LPJmL 4.0

The LPJmL 4.0 model (Lund-Potsdam-Jena managed Land, Schaphoff et al., 2018a, b), is a well established and validated process-based DGVM, which globally simulates the surface energy balance, water fluxes, carbon fluxes and stocks, and natural and managed vegetation from climate and soil input data. LPJmL simulates global vegetation distribution as the fractional coverage of plant functional types (PFT), which is called foliage projective cover (FPC), and managed land as fractional coverage of crop functional types (CFT). The establishment and survival of different PFTs is regulated through bioclimatic limits and effects of heat, productivity and fire on plant mortality. Therefore, it enables LPJmL to investigate feedbacks, for example between vegetation and fire. In standard settings, which are also used here, the model operates on the grid of $0.5° \times 0.5°$ lat-lon with a spinup time of 5000 years, repeating the first 30 years of the given climate data set.

Since its original implementation by Sitch et al. (2003), LPJmL has been improved by a representation of the water balance (Gerten et al., 2004), a representation of the agriculture (Bondeau et al., 2007), and new modules for fire (Thonicke et al., 2010), permafrost (Schaphoff et al., 2013) and phenology (Forkel et al., 2014).

Geosci. Model Dev. Discuss., https://doi.org/10.5194/gmd-2019-92
Manuscript under review for journal Geosci. Model Dev.
Discussion started: 2 May 2019

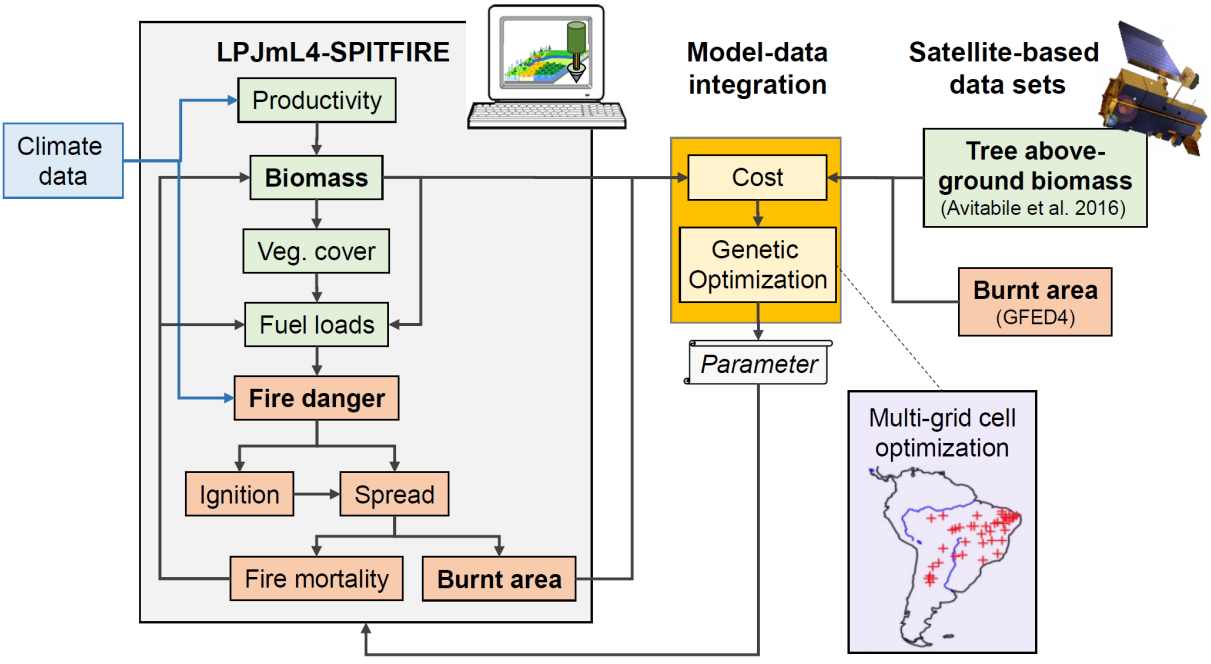

Figure 2. Schematic overview about the model-data integration approach to estimate parameters of LPJmL4-SPITFIRE against satellite-based data sets of burnt area and above-gorund biomass

2.1.2 SPITFIRE

SPITFIRE (SPread and InTensity of FIRE, Thonicke et al., 2010) is a process-based fire module, used in various vegetation models (e.g. Lasslop et al., 2014; Yue and Unger, 2018), including LPJmL4. We describe here its main features, which are published in Thonicke et al. (2010). SPITFIRE calculates fire disturbance by simulating the ignition, the danger, the spread and the effects of fire separately. As ignition sources SPITFIRE considers human ignition and lightning flashes. Human ignitions ($n_{h,ig}$) are a function of population density:

$$n_{h,ig} = P_D \cdot k(P_D) \cdot a(N_D)/100, \quad (1)$$

where

$$k(P_D) = 30.0 \cdot \exp(p_h \cdot \sqrt{P_D}). \quad (2)$$

P_D is the human population density (individuals km^{-2}) and $a(N_D)$ (ignitions individual^{-1} day^{-1}) describes the inclination of humans to cause fire ignitions (Eq. 3 and 4 in Thonicke et al., 2010). p_h is a parameter, which is set to -0.5 in Thonicke et al. (2010). This relationship assumes that human ignitions are lowest on very low populated regions and on high populated regions through a higher level of urbanization and landscape fragmentation. The ignition is highest for a medium-small population density. Lightning-caused ignitions are prescribed by lightning data from the OTD/LIS Gridded Climatological data set

Geosci. Model Dev. Discuss., https://doi.org/10.5194/gmd-2019-92
Manuscript under review for journal Geosci. Model Dev.
Discussion started: 2 May 2019

Geoscientific Model Development Discussions

(Christian et al., 2003), assuming that 20 % of the flashes reach the ground and their effectiveness to ignite a fire is 0.04. In the study area of South America human ignitions are by far the most dominant ignition source, due to missing lightning in the dry season.

Fire danger is by default computed by using the Nesterov index which accounts for the maximum and dew point temperatures as well as scaling factors for different PFTs on a daily time step. In the following section, we describe the calculation of the fire danger indices in detail (Sect. 2.2). Fire duration t_{fire} (min) is calculated as a function of the fire danger index, assuming that fires burn longer under a high fire danger:

$$t_{fire} = \frac{241}{1 + 240 \cdot \exp(p_d \cdot FDI)}, \tag{3}$$

where p_d is set to -11.06 in Thonicke et al. (2010). The maximum fire duration per day is 240 minutes.

The calculation of the forward rate of spread $ROS_{f,surface}$ (m min^{-1}) is based on the Rothermel equations (Rothermel, 1972; Pyne et al., 1996; Wilson, 1982):

$$ROS_{f,surface} = \frac{I_R \cdot \xi \cdot (1 + \Phi_w)}{\rho_b \cdot \epsilon \cdot Q_{ig}} \tag{4}$$

where I_R is the reaction intensity, ξ the propagation flux ratio, Φ_w a multiplier that accounts for the effect of wind, ϵ the effective heating number, Q_{ig} the heat of pre-ignition and ρ_b the fuel bulk density (Eq. 9 in Thonicke et al., 2010). ρ_b is a PFT dependent parameter and describes the density of the fuel, which is available for burning. It is weighted over the different fuel classes. Hence, a changing PFT distribution has an impact on the ROS.

The simulated fire ignitions, fire danger and fire spread are then used to calculate the burnt area, fire carbon emissions, and plant mortality. Plant mortality depends on the scorch height and the probability of mortality due to crown damage $P_m(CK)$. The scorch height SH describes the height of the flame at which canopy scorching occurs. It increases with the 2/3 power of the surface intensity $I_{surface}$:

$$SH = F \cdot I_{surface}^{0.667}, \tag{5}$$

where F is a PFT-dependent parameter. Assuming a cylindrical crown, the proportion CK affected by fire is:

$$CK = \frac{SH - H + CL}{CL}, \tag{6}$$

where H is the height of the average woody PFT and CL the crown length. The probability of mortality $P_m(CK)$ due to crown damage is then calculated by:

$$P_m(CK) = rCK \cdot CK^p, \tag{7}$$

where rCK is a PFT depended resistance factor between 0 and 1, and p in the range of 3 to 4. Disturbance by fire mortality has a large impact on the vegetation dynamics, which are calculated within LPJmL. SPITFIRE further includes a surface intensity threshold, which describes the threshold of the possible area burnt below which the surface intensity is set to zero and hence burnt area, emissions and fuel consumption is set to zero.

Geosci. Model Dev. Discuss., https://doi.org/10.5194/gmd-2019-92
Manuscript under review for journal Geosci. Model Dev.
Discussion started: 2 May 2019

SPITFIRE considers anthropogenic effects on fire by taking into account human ignitions but does not account for fire suppression. Only wildfires occurring in natural vegetation are simulated. Fire on managed land like agriculture or pasture areas is not implemented, which has to be taken into account if simulated burnt area is compared with satellite observation.

Furthermore, we introduced a small technical change in the LPJmL4 interaction with SPITFIRE compared to the original SPITFIRE implementation: In the version 4.0 of LPJmL the fire litter routine calculates the leaf and litter carbon pools in a daily time step. Since the LPJmL tree allocation works at a yearly time step, this implementation leads to an incorrect LPJmL4-SPITFIRE interaction. We now split the fire-litter routine into two parts; the first one allocates burnt matter into the litter at a daily time step without recalculating the pools and the second one calculates the leaf and root carbon pools at a yearly time step.

2.2 Fire danger indices

The fire danger index (FDI) is a key parameter within process-based fire models such as SPITFIRE. The FDI determines the probability and the intensity of a spreading fire, which impacts fire behaviour.

2.2.1 Nesterov index-based fire danger index (FDI_{NI})

The fire danger index within SPITFIRE is based on the daily (d) calculated Nesterov Index NI(d) (Venevsky et al., 2002), which is widely used in numeric fire simulations. The NI is a cumulative function of daily maximum temperature $T_{max}(d)$ and dew-point temperature $T_{dew}(d)$ ($^{\circ}C$) and set to zero at a precipitation $\geq$ 3 mm or a temperature $\leq 4\,^{\circ}C$:

$$NI(d) = \sum T_{max}(d) \cdot (T_{max}(d) - T_{dew}(d)), \tag{8}$$

$$T_{dew} = T_{min}(d) - 4. \tag{9}$$

The final FDI is then calculated by taking into account the Nesterov index as measure for the fire weather conditions, the total dead fuel load for the different fuel classes i (ω_{0_i}) and the moisture of extinction m_e, the latter is a PFT depended parameter and is weighted over the litter amount.

The fire danger index is scaled by a PFT-dependent constant, α_i, over the number of PFTs *n* (Thonicke et al., 2010):

$$FDI_{NI} = max\left(0, \left(1 - \frac{1}{m_e} exp\left(-\sum_{i=1}^{n} \alpha_i \cdot \frac{\omega_{0_i}}{\omega_0}\right) \cdot NI\right)\right). \tag{10}$$

We will use the scaling factors α_i in the parameter optimization (Sect. 2.4).

2.2.2 Vapor pressure deficit-based fire danger index (FDI_{VPD})

We implemented a new fire danger index, based on the water vapor pressure deficit (VPD). The VPD describes the difference of the saturation water vapor pressure e_s and the actual water vapor pressure in the air. For the parameterization of the VPD

Geosci. Model Dev. Discuss., https://doi.org/10.5194/gmd-2019-92
Manuscript under review for journal Geosci. Model Dev.
Discussion started: 2 May 2019

we used an approach based on Pechony and Shindell (2009):

$$VPD \propto 10^{Z(T)}(1 - RH/100), \tag{11}$$

where T is the air temperature, RH the relative humidity and Z the Goff-Gratch equation (Goff and Gratch, 1946) to calculate the saturation vapor pressure. The flammability F at time step *t* for each grid cell can then be expressed as:

$$F(t) = 10^{Z(T(t))}\left(1 - \frac{RH(t)}{100}\right) VD(t) e^{-c_R R(t)}, \tag{12}$$

where VD is the vegetation density, R the total precipitation in mm/day and c_R is a constant factor ($c_R = 2$ day/mm). Here we used the simulated FPC from LPJmL4 as a proxy for the VD and a monthly mean for R to avoid unrealistic high flammability fluctuations in time steps with isolated events of very low R. Based on this implementation in SPITFIRE, the resulting FDI was much smaller than the original FDI_{NI}. Hence, we scaled the VPD up with a PFT-dependent scaling factor α_i:

$$FDI_{VPD} = \frac{\sum \alpha_i \cdot FPC_i}{\sum FPC_i} \cdot F(t). \tag{13}$$

α_i for the FDI_{VPD} was not included in (Pechony and Shindell, 2009), but is important in order to allow different fire responses for different tree and grass types. We will use the scaling factors α_i in the parameter optimization (Sect. 2.4).

In comparison to the NI, the VPD requires more climate variables as input as it uses relative humidity and vegetation cover as additional fire-relevant variables. Vegetation cover has a direct link to fire risk by providing the number of available fuel for burning. According to many studies (e.g. Ray et al., 2005; Sedano and Randerson, 2014; Seager et al., 2015) the FDI_{VPD} is a very accurate fire danger index with a high correlation with fire occurrence, while still being relatively easy to implement in a global fire model.

The general behaviour of the two indices as modelled by LPJmL in dependence of relative humidity and temperature is shown in Fig. 3. The Nesterov index shows a strong but very localized maximum for high temperatures and a small humidity. The VPD on the other hand shows a less pronounced maximum but a medium fire danger also for wetter and colder regions. This might increase the area in which fires occur compared to the Nesterov index, which could be an important improvement, enabling SPITFIRE to simulate also more fire in wetter regions.

2.3 Model input data

LPJmL4-SPITFIRE requires input data on daily air temperature, precipitation, long-wave and shortwave downward radiation, wind and specific humidity, which we took from the NOAH Global Land Assimilation System (GLDAS, Rodell et al., 2004). The data has a spatial resolution of $0.25° \times 0.25°$ and the time step is 3 hours. We regridded and aggregated the data set to the LPJmL resolution of $0.5° \times 0.5°$ and to a daily time step. We used the GLDAS 2.0 for the years 1948-1999 and the version GLDAS 2.1 for the years 2000-2017. GLDAS 2.1 uses multiple satellite- and ground based observational data as well as advanced land surface modelling and data assimilation techniques. GLDAS 2.0 is forced entirely with the Princeton meteorological forcing data (Civil and Environmental Engineering/Princeton University, 2006). Because LPJmL4 requires at least 30 years of climate data for its spin-up (Sect. 2.1.1), the time span covered by GLDAS 2.1 is too short. To run the model, we used

Geosci. Model Dev. Discuss., https://doi.org/10.5194/gmd-2019-92
Manuscript under review for journal Geosci. Model Dev.
Discussion started: 2 May 2019

Geoscientific Model Development Discussions
Open Access
EGU

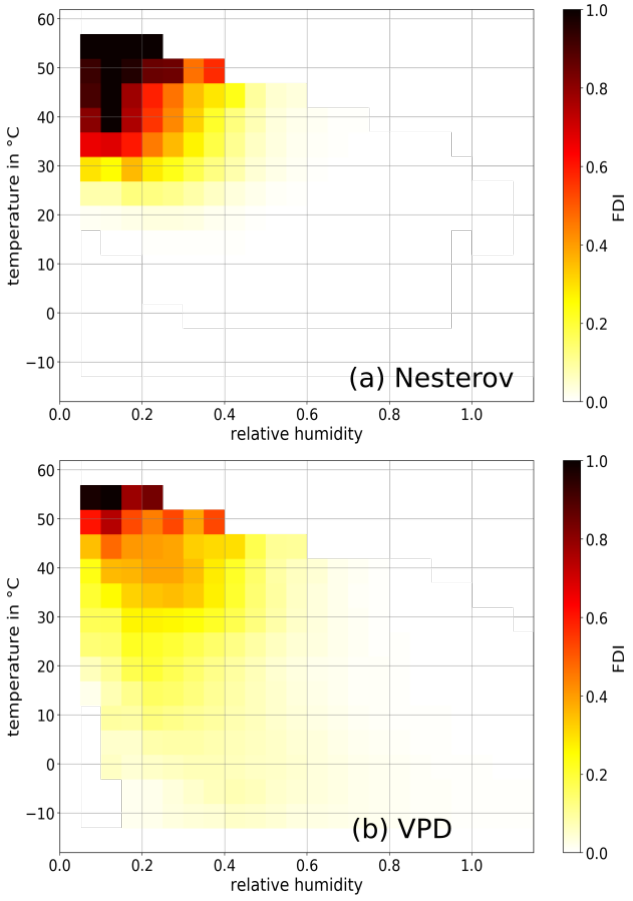

Figure 3. Dependence of the simulated fire danger index on monthly mean relative humidity and temperature for (a) the Nesterov-based index and (b) the VPD-based index. Both indices were calculated with monthly data for the years 2000-2010.

both climate data sets, but used the years 2003-2013 from GLDAS 2.1 for the optimization and 2005-2015 for the evaluation period.

Furthermore, LPJmL4-SPITFIRE is forced with gridded constant soil texture (Nachtergaele et al., 2009) and annual information on land use from Fader et al. (2010). Atmospheric CO_2 concentrations are used from Mauna Loa station (Quéré et al., 2015) and applied globally. The population density is taken form Goldewijk et al. (2011) and the lightning flashes are taken from the OTD/LIS satellite product (Christian et al., 2003).

2.4 Model optimization

To estimate parameters of LPJmL4-SPITFIRE, we aimed to calibrate model results against satellite observations of burnt area (GFED4: Giglio et al., 2013; Werf et al., 2017). However, as fire occurrence and spread impact and depend on vegetation productivity, hence fuel load, we wanted to ensure to not over-fit LPJmL4 against burnt area but to additionally achieve a re-

Geosci. Model Dev. Discuss., https://doi.org/10.5194/gmd-2019-92
Manuscript under review for journal Geosci. Model Dev.
Discussion started: 2 May 2019

Geoscientific Model Development Discussions

alistic vegetation distribution. Therefore, we additionally included a satellite-derived data set on above-ground biomass (AGB, Avitabile et al., 2016) of trees in the optimization. We combined burnt area and AGB with the corresponding model outputs within a joint cost function and applied a genetic optimization algorithm to estimate model parameters (Fig. 2). The implementation of the genetic optimization algorithm (Mebane and Sekhon, 2011) for LPJmL is described in (Forkel et al., 2014). The used cost function is based on the Kling-Gupta efficiency (KGE), which is the Euclidean distance in a three-dimensional space of model performance measures that account for the bias, ratio of variance and correlation between simulations and the observations. Gupta et al. (2009) showed that the KGE performs in an optimization setup better than e.g. the Nash-Sutcliffe efficiency (and hence MSE). We extended the KGE by defining it for multiple data sets d (i.e. burnt area and AGB):

$$Cost = \sqrt{\sum_{d=1}^{N}\left(\frac{\acute{s_d}}{\acute{o_d}}-1\right)^2+\left(\frac{\sigma_{s,d}}{\sigma_{o,d}}-1\right)^2+(r(s_d,o_d)-1)^2} \tag{14}$$

where $\acute{s}$ and $\acute{o}$ are mean values (bias component) over space (i.e. different grid-cells) and time (e.g. months) of simulations s and the observations o, respectively. σ_s and σ_o are variances (variance component) and r is the Pearson correlation coefficient over space and time. The optimization was performed for 40 grid-cells in South America to represent a variety of fire regimes (Fig. 2). Most of them were selected in active fire regions, especially in the Cerrado and Caatinga. In addition a few pixels with no or almost no fire occurrence (e.g. central Brazilian Amazon) were chosen.

Several parameters of LPJmL4-SPITFIRE were included in the optimization that cover different fire processes: ignition (human ignition parameter p_h, Eq. 2), fire danger (scaling factors FDI (α_i), Eq. 10 and 13), fire spread (fire duration p_d, Eq. 3), fuel bulk density (ρ_b, Eq. 4), surface intensity threshold and fire effects (scorch height parameter F, Eq. 5; crown mortality parameter rCK, Eq. 7). While p_d, p_h and the surface intensity threshold are global parameters (for all PFTs), the others were optimized for each PFT separately. Since we focus here on tropical South America, we used tropical broadleaved evergreen (TrBE), tropical broadleaved raingreen (TrBR) and tropical herbaceous (TrH) PFTs for the optimization.

The comparison of the two presented fire danger indices is the main objective of this study. Hence the optimization of the PFT-dependend FDI scaling factors α_i is very important and for the VPD obligatory because of no prior values. Accordingly, we conducted two different optimization experiments using LPJmLmdi: First, using the VPD as FDI (VPD_{optim}) and secondly using the Nesterov index as FDI (NI_{optim}). Both resulting parameter sets were then used for a corresponding LPJmL4 run and were compared to the unoptimized original model version using the NI (NI_{orig}) and various evaluation data sets.

2.5 Evaluation data

We used burnt area from the global fire emission database (GFED4; Giglio et al., 2013; Werf et al., 2017), in the model optimization and to evaluate model results. The global data set is available at a resolution of $0.25° \times 0.25°$ in a monthly time step from 1997 until 2016. The GFED burnt area product is based on the 500 m Collection 5.1 MODIS direct broadcast (DB) burnt area product (MCD64A1, after 2001). We used data for the years 2003-2013 in the optimization in order to not include potential inconsistencies between the GLDAS 2.0 and 2.1 climate data sets or between burnt area observations within GFED that originate from different satellite sensors. The GFED product comes with a stratification of burnt area by land cover from

Geosci. Model Dev. Discuss., https://doi.org/10.5194/gmd-2019-92
Manuscript under review for journal Geosci. Model Dev.
Discussion started: 2 May 2019

the MODIS land cover map in the resolution of 500 m (Giglio et al., 2013). As LPJmL does not simulate fire on managed lands, we excluded burnt area on cropland classes from model-data comparisons. To constrain the simulated vegetation distribution, we used the AGB data set from Avitabile et al. (2016). This data set is approximately representative for the late 2000s and therefore we compared it against simulated AGB for the years 2009-2011. We regridded all data set to a $0.5° \times 0.5°$ resolution. In addition, we used maps of PFTs as derived from the ESA CCI land cover map V2.0.7 (Li et al., 2018; Forkel et al., 2014).

2.6 Evaluation metrics

To quantify the performance of the model output, we applied the Pearson Correlation between two time series, the normalized mean square error (NMSE; Kelley et al., 2013) and the Willmott coefficient of agreement (W; Willmott and Willmott, 1982) to describe differences between the model simulation and the reference data sets. The NMSE is calculated by:

$$NMSE = \frac{\sum_{i=1}^{N}(y_i - x_i)^2}{\sum_{i=1}^{N}(x_i - \bar{x})^2} \tag{15}$$

where y_i is the simulated and x_i the observed value in the grid cell i. $\bar{x}$ is the mean observed value. The NMSE is zero for perfect agreement between simulated and modelled results, 1.0 if the model is as good as using the observed mean as a predictor and larger than 1.0 if the model performs worse than that. The Willmott coefficient of agreement is given by:

$$W = 1 - \frac{\sum_{i=1}^{N}(y_i - x_i)^2 \cdot A_i}{\sum_{i=1}^{N}(|y_i - \bar{x}| + |x_i - \bar{x}|)^2 \cdot A_i} \tag{16}$$

which additionally accounts for the area weight A_i of the grid cell i.

3 Results

3.1 Performance of optimized fire danger index formulations

Overall, the yearly burnt area simulated by the standard SPITFIRE model (using the original Nesterov index, NI_{orig}) showed poor simulations results over South America as compared to the GFED4 evaluation data set (Fig. 4 a and b: NMSE=1.80, W=0.27). The average yearly burnt area (without croplands) for South America was with ca. 14 million *ha* about 25 % smaller than the observed burnt area with 19 million ha in the shown period from 2005-2015. The spatial pattern of the modelled burnt area agreed well with the GFED4 data around the Cerrado/Caatinga border, while the fires in other semi-arid regions of the continent were underestimated. For example, simulated fire is underestimated in the savanna-areas in the northern part of South America (on the Columbian-Venezuelian border) even though there is a strong signal visible in the satellite observations. The biomes Caating and Cerrado, which are of special interest in this study, showed very different results: while fire in Caatinga was underestimated, it was overestimated in the Cerrado. The optimized version using NI_{optim} (Fig. 4 d), led to an overall decrease of fire, with a slight improvement of NMSE (1.09) as compared to NI_{orig} and a worse Willmott coefficient of 0.08. While the overestimation of fire in Caatinga was reduced, all the fires across South America also have decreased significantly, which led to a general underestimation of fire by 90 % (2 million ha).

Geosci. Model Dev. Discuss., https://doi.org/10.5194/gmd-2019-92
Manuscript under review for journal Geosci. Model Dev.
Discussion started: 2 May 2019

Geoscientific Model Development Discussions

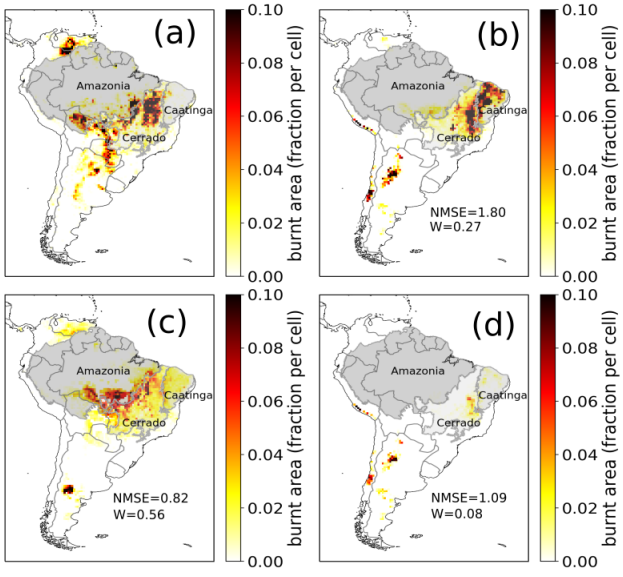

Figure 4. Yearly burnt area over a mean from 2005-2015 as fraction per cell. (a) GFED4 evaluation data of burnt area excluding crops and simulated burnt area by SPTIFIRE using the (b) NI_{orig} version, (c) VPD_{optim} version, (d) NI_{optim} version

The optimized version, using VPD_{optim} (Fig. 4 c), clearly improved the model performance, mainly by shifting much of the simulated burnt area from the sparsely vegetated Caatinga towards the Cerrado region (NMSE=0.82 and W=0.56). In addition, by using VPD_{optim}, the model results also showed fire occurrence in northern South America, where fire was not at all or only minimally simulated when using NI_{optim} or NI_{orig}. The total burnt area was in this model version ca 20 % smaller than the evaluation data set (16 million ha).

The burnt area time series from 2005 to 2015 provides a more detailed view on the model performance for the fire-prone Cerrado and Caatinga region (Fig. 5). While model performance was relatively good for the Cerrado region with NI_{orig} (NMSE=0.3, W=0.89, R^2=0.78), the simulated burnt area was strongly overestimated in the Caatinga region throughout the whole period (NMSE=327.82, W=0.14, R^2=0.59). After the optimization of the NI, the model performance indeed improved for the Caatinga (NMSE=1.07, W=0.73, R^2=0.31), but at the same time the performance for the Cerrado got much worse (NMSE=1.07, W=0.36, R^2=0.4). On the other hand VPD_{optim} showed an improved fire representation compared to the standard settings in the Cerrado (NMSE=0.27, W=0.9, R^2=0.8) as well as in the Caatinga (NMSE=15.2, W=0.46, R^2=0.56). Even though fire in the Caatinga was still overestimated, the NMSE decreased by a factor of six.

Overall, the total amount of burnt area in the Cerrado was for all three model versions smaller than in the evaluation data set. Fire occurrence in the Caatinga was, on the other hand, largely overestimated by the NI_{orig} and the VPD_{optim} version. Just in the NI_{optim} version the burnt area of the Caatinga is in the same order of magnitude as the evaluation data set, which also led, however, to a large underestimation in the Cerrado (Tab. 1).

Geosci. Model Dev. Discuss., https://doi.org/10.5194/gmd-2019-92
Manuscript under review for journal Geosci. Model Dev.
Discussion started: 2 May 2019

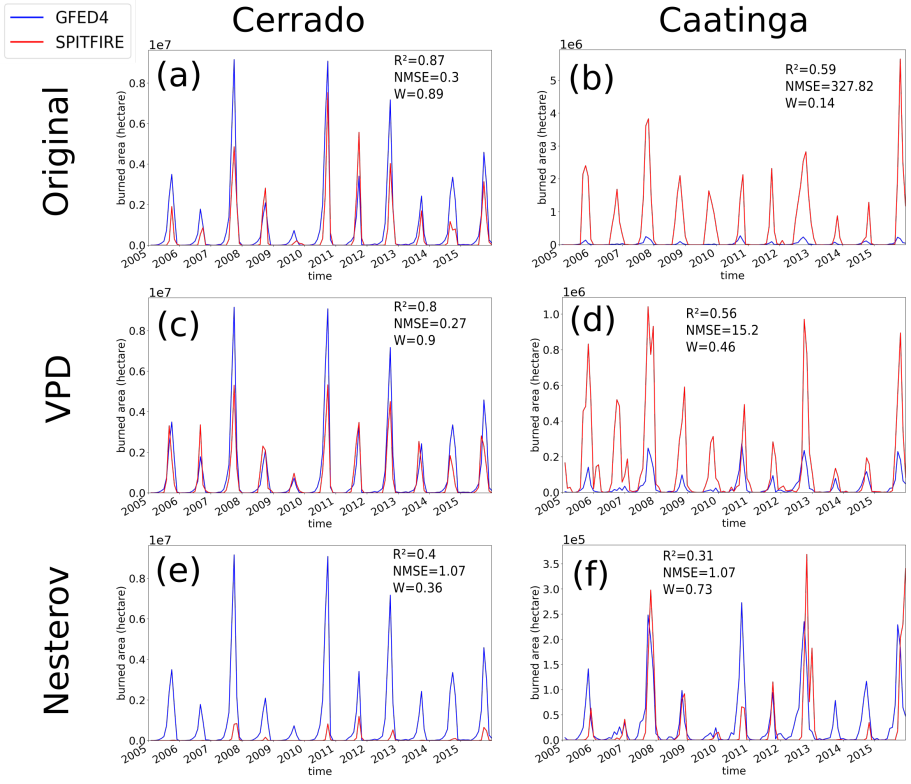

Figure 5. Timeseries of monthly burnt area from 2005 - 2015 simulated by SPITFIRE (red lines) compared to GFED4 evaluation data (blue lines) for: (a) The Cerrado region, using NI_{orig}. (b) The Caatinga region, using the NI_{orig}. (c) The Cerrado region, using VPD_{optim}. (d) The Caatinga region, using VPD_{optim}. (e) The Cerrado region, using NI_{optim}. (f) The Caatinga region, using NI_{optim}. Note different scale for each Figure.

3.2 Optimized model parameters

Seven fire-related parameters were optimized, in order to improve the fire representation in the LPJml4-SPITIFRE model. Here we compare the optimized parameters for the different model versions in order to evaluate and discuss parameter variability and changes. Table 2 shows all parameters, used for the optimization, their lower and upper boundary and the resulting optimized value. Since the FDI directly controls the amount of modelled fire, the FDI scaling factors for the different PFTs are central for this analysis. For both optimization experiments the boundaries were, hence, set rather generously within one magnitude of the original value. In the NI_{optim} experiment, all scaling factors generally decreased compared to the standard values used for NI_{orig}. Here, TrH displayed the smallest scaling factor ($9.39 \cdot 10^{-6}$), followed by TrBE ($2.48 \cdot 10^{-5}$) and TrBR ($4.76 \cdot 10^{-5}$). Since the VPD is a newly implemented fire danger index, we have no standard values to compare the optimized scaling factors with. Here, the TrBE showed the largest value (22.41), ca. 20 times as large as the TrBR (1.21) and TrH (1.13) (Tab. 2).
In case of the other optimized parameters the boundaries were set smaller in order to decrease the possibility that a large error

Geosci. Model Dev. Discuss., https://doi.org/10.5194/gmd-2019-92
Manuscript under review for journal Geosci. Model Dev.
Discussion started: 2 May 2019

Geoscientific Model Development Discussions

Table 1. Comparison of the results in terms of NMSE, the Willmott coefficient of agreement and the sum (in ha per year) between NI_{orig}, VPD_{optim}, NI_{optim} and the GFED evaluation data

Region	NMSE	Willmott	Sum
Spatial - South America			
GFED			$1.9 \cdot 10^7$
NI_{orig}	1.80	0.27	$1.4 \cdot 10^7$
VPD_{optim}	0.82	0.56	$1.6 \cdot 10^7$
NI_{optim}	1.09	0.08	$0.2 \cdot 10^7$
Temporal - Cerrado			
GFED			$9.2 \cdot 10^6$
NI_{orig}	0.30	0.89	$5.2 \cdot 10^6$
VPD_{optim}	0.27	0.90	$6.4 \cdot 10^6$
NI_{optim}	1.07	0.36	$0.6 \cdot 10^6$
Temporal - Caatinga			
GFED)			$0.4 \cdot 10^6$
NI_{orig}	327.82	0.14	$6.0 \cdot 10^6$
VPD_{optim}	15.2	0.46	$1.6 \cdot 10^6$
NI_{optim}	1.07	0.73	$0.3 \cdot 10^6$

in the estimation of several parameters would lead to a better overall cost in the optimization procedure. The human ignition parameter became smaller for both optimizations, which led to a smaller amount of human ignitions (from -0.5 to -0.54 in NI_{optim} and -0.53 in VPD_{optim}). The fuel bulk density increased for all three tropical PFTs in the NI_{optim} version, while for VPD_{optim} the fuel bulk density of the TrBE and TrH PFTs decreased and for the TrBR increased. For the NI_{optim} version, the fire duration parameter (p_d) increased, leading to a shorter fire duration (from -11.06 to -9), while the value for the VPD_{optim} version stayed relatively similar (-11.37) to the prior value. The surface intensity threshhold became slightly larger for the NI_{optim} version than the original value (from 10^{-6} to $1.03 \cdot 10^{-6}$). For VPD_{optim} the parameter increased by a factor of three ($3.63 \cdot 10^{-6}$). The mortality related parameters F and rCK led in the NI_{optim} version both to a decrease in the fire-related mortality for TrBE and an increase for TrBR PFTs. The optimized parameters for VPD_{optim} led to a decrease in the fire related mortality for both PFTs.

The relative uncertainties were for most optimized parameters very small (between 0 and 0.05), hence these parameters were strongly constrained (Fig. 6). Just the fire-mortality related parameters (F and rCK) had large uncertainties for the TrBR, hence weakly constrained. For VPD_{optim} the uncertainty of rCK (TrBR) was 0.8 and for NI_{optim} the uncertainty of F was 0.9 and for rCK 1 (TrBR).

Geosci. Model Dev. Discuss., https://doi.org/10.5194/gmd-2019-92
Manuscript under review for journal Geosci. Model Dev.
Discussion started: 2 May 2019

Geoscientific Model Development Discussions
Open Access
EGU

Table 2. All optimized parameters with their standard values, the upper and lower boundary of the parameter ranges and the resulting optimized value including parameter for specific PFTs and global parameter, which have the same value for all PFTs.

Parameter	PFT	Standard value (as in Thonicke et al., 2010)	Lower bound.	Upper bound.	After optimization
NI$_{optim}$					
scaling factor FDI α_i	TrBE	$3.34 \cdot 10^{-5}$	$7 \cdot 10^{-6}$	$1.33 \cdot 10^{-4}$	$2.4885 \cdot 10^{-5}$
scaling factor FDI α_i	TrBR	$3.34 \cdot 10^{-5}$	$7 \cdot 10^{-6}$	$1.33 \cdot 10^{-4}$	$4.7649 \cdot 10^{-5}$
scaling factor FDI α_i	TrH	$6.67 \cdot 10^{-5}$	$7 \cdot 10^{-6}$	$1.33 \cdot 10^{-4}$	$9.3949 \cdot 10^{-6}$
fire duration parameter p_d	all PFTs	-11.06	-13	-9	-9.0011
scorch height parameter F	TrBE	0.1487	0.01	0.6	0.1282
scorch height parameter F	TrBR	0.061	0.01	0.6	0.0752
crown mortality parameter rCK	TrBE	1.0	0.5	1	0.5030
crown mortality parameter rCK	TrBR	0.05	0	0.5	0.4038
fuel bulk density ρ_b	TrBE	25.0	22.5	27.5	26.6473
fuel bulk density ρ_b	TrBR	13.0	11.7	14.3	13.1896
fuel bulk density ρ_b	TrH	2.0	1.8	2.2	2.0019
human ignition parameter p_h	all PFTs	-0.5	-0.6	-0.4	-0.5426
surface intensity threshold	all PFTs	10^{-6}	10^{-7}	10^{-5}	$1.0317 \cdot 10^{-6}$
VPD$_{optim}$					
scaling factor FDI α_i	TrBE	-	1	50	22.4181
scaling factor FDI α_i	TrBR	-	1	50	1.2135
scaling factor FDI α_i	TrH	-	1	50	1.1299
fire duration parameter p_d	all PFTs	-11.06	-13	-9	-11.3753
scorch height parameter F	TrBE	0.1487	0.01	0.6	0.1930
scorch height parameter F	TrBR	0.061	0.01	0.6	0.0799
crown mortality parameter rCK	TrBE	1.0	0.5	1	0.9983
crown mortality parameter rCK	TrBR	0.05	0	0.5	0.4801
fuel bulk density ρ_b	TrBE	25.0	22.5	27.5	22.5923
fuel bulk density ρ_b	TrBR	13.0	11.7	14.3	13.3750
fuel bulk density ρ_b	TrH	2.0	1.8	2.2	1.8944
human ignition parameter p_h	all PFTs	-0.5	-0.6	-0.4	-0.5332
surface intensity threshold	all PFTs	10^{-6}	10^{-7}	10^{-5}	$3.6317 \cdot 10^{-6}$

Geosci. Model Dev. Discuss., https://doi.org/10.5194/gmd-2019-92
Manuscript under review for journal Geosci. Model Dev.
Discussion started: 2 May 2019

Geoscientific Model Development Discussions
Open Access
EGU

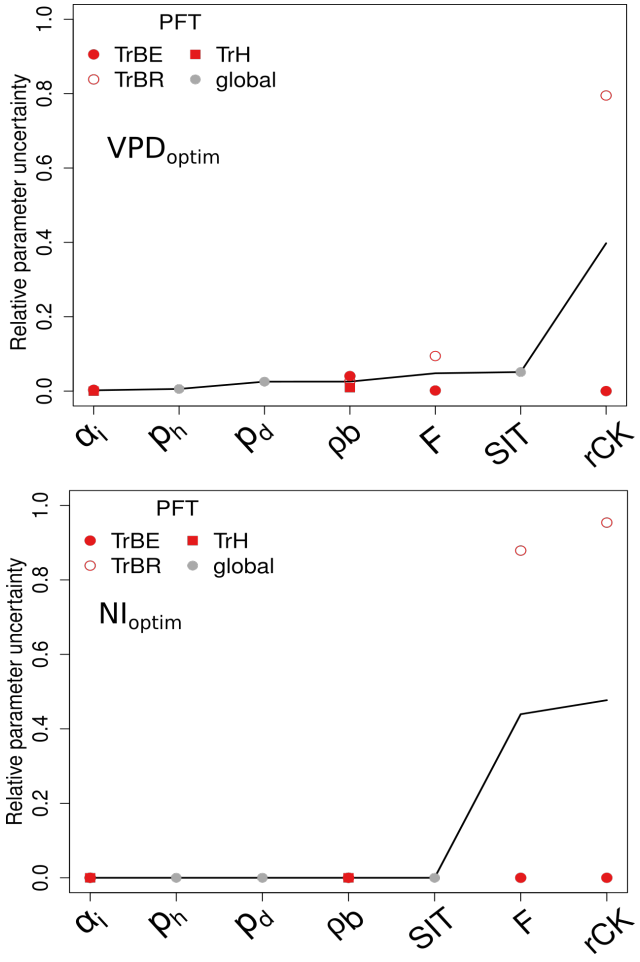

Figure 6. Relative uncertainty of model parameters after optimization for (a) VPD_{optim} and (b) NI_{optim}. The relative uncertainty is the ratio of the uncertainty after the optimization (range of all parametersets with low cost, below the 0.05 quantile) divided by the uncertainty before the optimization (range of the parameters for the optimization). Low and high values of relative uncertainty indicate strongly and weakly constrained parameters, respectively. All parameters are defined by PFT (red dots) or global (grey dots). The black lines are added to support visual interpretation and show the relative uncertainty of each parameter. SIT denotes the surface intensity threshold.

3.3 Model evaluation for South America

The modelled above-ground biomass (AGB) of trees in South America was throughout all model versions larger than the evaluation data set indicates (Fig. 7). Especially the Amazon region is with an average of ca. 20 kgC/m^2 about one third overestimated. The drier savanna regions on the continent yielded a biomass of ca. 5-10 kgC/m^2, which also constitutes an overestimation in wide parts of the Cerrado and the Caatinga biome (evaluation data shows between 1-5 kgC/m^2, also see Roitman et al., 2018).

Geosci. Model Dev. Discuss., https://doi.org/10.5194/gmd-2019-92
Manuscript under review for journal Geosci. Model Dev.
Discussion started: 2 May 2019

Geoscientific Model Development Discussions

Table 3. Comparison of the results for AGB and the TrBE PFT cover in terms of NMSE and the Willmott coefficient of agreement between NI_{orig}, VPD_{optim} and NI_{optim} in South America (SA) and in the Cerrado.

Region	NMSE	Willmott
AGB		
SA (NI_{orig})	0.97	0.83
SA (VPD_{optim})	0.91	0.84
SA (NI_{optim})	0.99	0.83
Cerrado (NI_{orig})	15.06	0.25
Cerrado (VPD_{optim})	12.36	0.28
Cerrado (NI_{optim})	16.06	0.24
FPC - Evergreem (TrBE)		
SA (NI_{orig})	0.42	0.82
SA (VPD_{optim})	0.41	0.82
SA (NI_{optim})	0.43	0.81
Cerrado (NI_{orig})	1.04	0.60
Cerrado (VPD_{optim})	0.70	0.64
Cerrado (NI_{optim})	1.40	0.55

The differences among the different model versions are marginal: The VPD_{optim} version had the best performance compared to the evaluation data set (NMSE= 0.91, W=0.84), the NI_{orig} version had the second best performance (NMSE=0.97, W=0.84) and the NI_{optim} the worst performance (NMSE=0.99, W=0.83). The model optimization scheme focuses on fire parameter, hence the model performance can only improve in fire-prone biomes, i.e. not in, e.g., wet tropical forest where fire is absent. In the fire-prone Caatinga and Cerrado the VPD_{optim} version mostly decreased the biomass by up to 3 kgC/m^2, showing a better performance compared to the evaluation data set (e.g. in the Cerrado the NMSE decreased from from 15.06 to 12.36 in the VPD_{optim} version compared to NI_{orig} see Tab. 3). The modelled foliage projective cover (FPC) showed for all three model versions a strong underestimation compared to the evaluation data set of the TrBE throughout the whole Amazonian region (ca. 50% compared to ca. 100% in the evaluation dateset). In the fire-prone biomes Cerrado and Caatinga, however, the TrBE PFT was sometimes overestimated (TrBE cover between 0 and 40 %, Fig. 8). In the regions with less TrBE the dominant PFT was mostly TrBR (Cerrado) or TrH (Caatinga).

NI_{optim} led to an overall decrease in the model performance also in terms of FPC, as both, the NMSE and the Willmott coefficient worsened compared to NI_{orig} (NI_{orig}: NMSE=0.42, W=0.82; NI_{optim}: NMSE=0.43, W=0.81).

The VPD_{optim} version, on the other hand, showed an slightly improved FPC distribution (NMSE=0.41, W=0.82) but also here we got an even larger improvement, when only the fire-prone regions Cerrado or Caatinga are considered (Tab. 3).

Geosci. Model Dev. Discuss., https://doi.org/10.5194/gmd-2019-92
Manuscript under review for journal Geosci. Model Dev.
Discussion started: 2 May 2019

Geoscientific Model Development Discussions

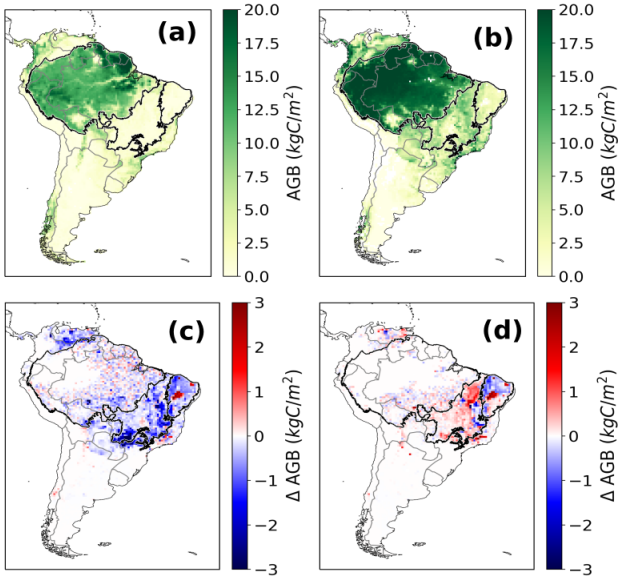

Figure 7. Annual above ground biomass (AGB) of trees over a mean from 2005-2015 in kgC/m^2. (a) Avitabile evaluation data. (b) Simulated AGB by LPJmL4-SPITFIRE in the NI$_{orig}$ version. (c) Difference between VPD$_{optim}$ and NI$_{orig}$. (d) Difference between NI$_{optim}$ and NI$_{orig}$. Red (blue) color indicates a larger (smaller) biomass after the optimization.

4 Discussion

In summary, our results show that the implementation of a new fire danger index based on the water vapor pressure deficit FDI_{VPD} and its optimization against satellite data sets improved the simulations of fire in LPJmL4-SPITFIRE, both in terms of spatial patterns as well as temporal dynamics of burnt area. In the following, we discuss the model improvements, limitations and recommendations for future improvements of process-based global fire models within the DGVM framework.

4.1 Improvements in model performance

The VPD results showed a better model performance for fire in the spatial dimension, as well as in the temporal dimension (Tab. 1 and 3). Compared to the Nesterov index, FDI_{VPD} uses additional climate input as relative humidity and precipitation. In the calculation of the Nesterov index precipitation is just used as a threshold. This leads to a better accounting of the very different climatic conditions among various biomes. Furthermore, the FDI_{VPD} includes a direct representation of the vegetation density. The significante of this has been recently shown by findings of Forkel et al. (2019) who have emphasized the importance of past plant productivity and fuel production for burnt area. This is particular important for differentiating between fires in biomes with similar PFT distribution. For example, the vegetation density is much higher in the Cerrado, even though the Caatinga and Cerrado have a similar modelled PFT composition. A larger VD provides more fire fuel and therefore

Geosci. Model Dev. Discuss., https://doi.org/10.5194/gmd-2019-92
Manuscript under review for journal Geosci. Model Dev.
Discussion started: 2 May 2019

Geoscientific Model Development Discussions
Open Access
EGU

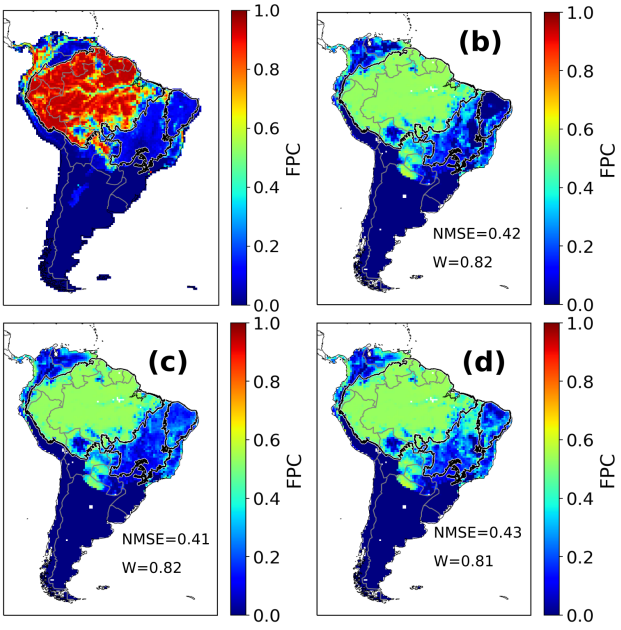

Figure 8. Annual FPC cover by tropical broadleaved evergreen PFT over a mean from 2005-2015 as fraction per cell. (a) ESA-CCI evaluation data (b) Simulated FPC by LPJmL4-SPITFIRE using the NI_{orig} version (c) Simulated FPC by LPJmL4-SPITFIRE using the VPD_{optim} version (d) Simulated FPC by LPJmL4-SPITFIRE using the NI_{optim} version

leads to a higher fire danger.

While the seasonal and interannual variability in the Caatinga has improved largely using the FDI_{VPD} (NMSE decreased by a factor of ca. 20), the improvement in the Cerrado was relatively small (NMSE decreased by ca. 10%). This is due to the fact, that the optimization tries to obtain a compromise between the different optimized cells. As the model performance was originally much better for the Cerrado, the largest improvement could be achieved for the Caatinga. We have also chosen a large amount of cells in the Caatinga, because the model performance was here particular bad. This leads to a large improvement in the time series of the Caatinga region, while the improvement for the Cerrado was less significant.

Another result of the optimizing procedure, using FDI_{VPD}, was the improvement of the PFT distribution and the above-ground biomass of trees especially in the fire-prone biomes Caatinga and Cerrado (Fig. 8). The Amazon, where fire is a scarce event, shows almost no changes compared to the non-optimized model version. Here, it is the improvement of the vegetation model itself, and not the fire module, which can help to improve the model performance of LPJmL4-SPITFIRE. Hence, it emphasizes that three parameter sets determining PFT distribution, biomass and fire are required in the optimization to obtain a realistic spatial and temporal distribution of both, vegetation and fire. It becomes especially visible in semi-arid, hence fire-prone biomes, where vegetation dynamics and fire are strongly coupled.

During the optimization-process most of the optimized parameters were well constrained, except for the mortality-related parameters for the TrBR PFT. The TrBR PFT is dominant in the fire-prone regions, where the mortality-related parameters

have a large impact on vegetation dynamics. Hence, they impact multiple LPJmL routines, which are responsible for the PFT distribution and carbon cycling. This leads in turn to a less certain parameter estimation. In order to better constrain these parameters also the optimization of vegetation model parameters would be an approach to decrease the uncertainties.

4.2 Limitations during the optimization process

Fire largely depends on the vegetation type and their associated flammability, fire tolerance and mortality. Hence an accurately modelled vegetation distribution is crucial for a good model performance in terms of burnt area and fire effects (Forkel et al., 2019; Rogers et al., 2015). As shown in Fig. 8, the modelled PFT coverage showed an equal distribution of tropical raingreen and evergreen PFTs throughout wide parts of central-northern South America. Evaluation data shows, however, an evergreen dominance in the wet rainforest regions and a raingreen dominance in the Cerrado and Caatinga. By choosing a large amount of optimization cells in the, by NI_{orig}, strongly overestimated Caatinga region, the burned area decreased there significantly after the optimization. Because the modelled proportion of tropical evergreen trees in the Cerrado is similar to the Caatinga biome, fire occurrence in the Cerrado has also over-proportional decreased for NI_{optim} (Fig. 4). As a result the modelled fire in whole South America was rather low, which improved the performance in the Caatinga but decreased it in other regions.

Even though the VPD suffers from the same limitations, its optimized version has indeed improved simulated fire in wide parts of South America (including both Caatinga and Cerrado) and led to a better overall model performance for South America in terms of burnt area, biomass and PFT distribution. The reason for this behaviour is the above discussed impact of vegetation density and the more comprehensive representation of the climate impact. This emphasizes the potential of the VPD to be used as the standard fire danger index in SPITFIRE and to improve the fire modelling even further, based on a possible improved PFT distribution. In the tropical rainforest the modelled TrBE proportion should be much larger. In the Cerrado and especially the Caatinga, however, trees suffer from water stress in the dry season and should shed their leaves to avoid mortality related to drought or growth efficiency. The resulting dominance of the TrBR PFT has a very different effect on fire spread and is more fire-tolerant (different fuel characteristics and resulting fire intensity), thus has a lower fire-related mortality.

As stated before, the VPD fire danger index requires additional climate variables which are available from re-analysis data. We have chosen the GLDAS climate data set for its good performance to capture South-American climate. Because GLDAS 2.0 (covering 1948-2010) is just forced with Princeton meterological data, while GLDAS 2.1 (2000-now) includes various observational and meteorological data, both versions result in a small offset. Since the offset is very small, the years 2000-2003 (first three years of GLDAS 2.1, before the optimization period) are enough for the model to recover from the offset and the carbon pools to return to equilibrium. To exclude the possibility that long-term trends within GLDAS 2.0 changed the modelled vegetation state significantly, we tested our optimization also just based on GLDAS 2.0 data (until 2010) and just based on GLDAS 2.1 data (2000-2017), using the same years for model spinup, optimization and evaluation. Both versions yielded similar results compared to the optimization presented in this study (results not shown).

Due to the fact that evaluation data are only available for the last 10-20 years, we are constrained to optimize the model in this relatively short time period. In South America these years were subject to an unusual high amount of severe droughts and other extreme events (Panisset et al., 2017). As a result, an optimization in this period could lead to a worse model performance in a

period with less pronounced droughts. This is due to the non-linear relationship between the drought signal in the input data set and the resulting modelled biosphere behaviour. Nonetheless, we were able to improve the interannual variability and hence, the model performance during extreme years for the Cerrado and Caatinga regions (e.g. for 2007/2008, Fig. 5). The optimized SPITFIRE is now able to model accurately the climate dependent seasonal and interannual variability as well as the spatial extent of fire on natural land throughout the fire-prone woodlands of South America.

4.3 Outlook - the way ahead in improving fire modules in DGVMs

In fire-prone regions the interactions between fire and vegetation dynamics is strong, hence posing a challenge for global fire models embedded in DGVMs. By just focussing on fire-related parameter, an optimization approach can only to a certain extent additionally improve PFT distribution and simulated biomass. For a good fire representation e.g. in the Cerrado and Caatinga, a shrub PFT could further improve the model performance. Most fires in this region occur, where shrub PFTs are abundant. LPJmL tries to account for this by establishing rather small raingreen PFTs as a shrub replacement. A much better option would be a seperate shrub PFT with parameters leading to a high flammability, but also a low fire mortality. An optimization of LPJmL4-SPITFIRE, including shrub PFTs could yield much better results than shown in this study.

Even though the VPD is more complex than the Nesterov index and takes into account more climatic input, it would be possible to use an even more comprehensive fire danger index (e.g. Canadian Fire Weather Index; Wagner et al., 1987) or different fire danger indices for different biomes. There are various other fire danger indices used for modelling purposes, as well as real fire danger assessment and fire forecast purposes. For example, fire-prone countries have developed their own fire danger indices (e.g. Canada, Australia), which are suited to the unique local fire regimes and vegetation dynamics. In a global modelling approach, however, we need to find one fire danger index, which suits best for all regions of the world and has a relatively easy implementation to decrease computational cost and the number of input data sets (which might be unavailable or uncertain).

Currently, SPITFIRE does not account for fire in managed land like cropland or managed grassland. We accounted for this by excluding cropland fires from the evaluation burnt area data set. We do, however, not account for the proportion of grassland, which is used for e.g. cattle ranching. Since in SPITFIRE fire is not enabled on managed grassland, our results show a slightly smaller fire amplitude throughout South America than could be expected with managed land included and hence also compared to the GFED4 evaluation data set. The reason and timing of using fire on managed land depends less on climatic factors but mostly on social and political decisions, which vary among different countries, as well as different regions within e.g. Brazil. With fires on managed land included we would expect to further improve the simulated interannual variability.

5 Conclusions

We have demonstrated a major improvement of the fire representation within LPJmL4-SPITFIRE by implementing a new fire danger index and applying a model-data integration setup to optimize fire-related parameters. We improved the seasonal and interannual variability, as well as the spatial pattern of burnt area in South America. In addition, modelling of related vegetation variables, e.g., the biomass and the PFT distribution in the fire-prone Cerrado and Caatinga biomes have also been improved.

To our knowledge this is the first study that attempts to systematically optimize a process-based fire model within a complex DGVM. E.g. Rabin et al. (2018) did an optimization of a fire model, which is not embedded in a DGVM.

Optimizing fire parameter has its limits due to error propagation of the PFT distribution and hence their fire traits influencing simulated fire spread and behaviour. Furthermore, it remains a challenge to find a fire danger index that is physically interpretable and can be applied globally. In this study, the parameter-optimization by using FDI_{NI} led to a large underestimation of fire and a generally worse model performance, when focusing on the Cerrado and Caatinga biome. However, implementing the more complex FDI_{VPD} and optimizing it thereafter, led to an improved model performance compared to the original SPITFIRE implementation for South America. Our results demonstrate that the improvement of model processes, as well as a systematic model-data optimization are required in order to obtain a more accurate fire representation within complex DGVMs, where observations or experimental evidence to constraint fire parameter is scarce. This work highlights the potential for future model-data integration approaches to obtain a better fire model performance in a global setting, based on improved vegetation dynamics within LPJmL4. A realistic representation of fire is also crucial for fire-vegetation-climate feedbacks and is hence necessary for DGVMs coupled within an comprehensive Earth system model.

Code availability. Upon request. With publication of this article the model code will be published at https://github.com/PIK-LPJmL, analogously to Schaphoff et al. (2018a).

Author contributions. MD, MF and KT designed the study in discussion with MC, MB, BS and JK. MD and MF implemented the model-data integration framework for LPJmL4. MD and WvB implemented the new fire danger index. MD performed the analysis with inputs form MF. MD wrote the paper with inputs from all Co-authors.

Competing interests. The authors declare that they have no conflict of interest.

Acknowledgements. This paper was developed within the scope of the IRTG 1740 / TRP 2015/50122-0, funded by the DFG / FAPESP (MD und KT). MC acknoledges the support from the projects FAPESP 2015/50122-0 (São Paulo Research Foundation), and CNPq 314016/2009-0 (Brazilian National Council for Scientific and Technological Development). MF acknowledges funding through the TU Wien Wissenschaftspreis 2015. MB acknowledges the support of the Brazilian Research Network on Global Climate Change (Rede Clima) and of the National Institute of Science and Technology for Climate Change Phase 2 under CNPq, Grant 465501/2014-1, FAPESP, Grant 2014/50848-9 and the National Coordination for High Level Education and Training (CAPES) Grant, 16/2014. KT and BS acknowledge funding from the BMBF- and Belmont Forum-funded project "CLIMAX: Climate Services Through Knowledge Co-Production: A Euro-South American Initiative For Strengthening Societal Adaptation Response to Extreme Events", Grant no. 01LP1610A.

References

Alvares, C. A., Stape, J. L., Sentelhas, P. C., de Moraes Gonçalves, J. L., and Sparovek, G.: Köppen's climate classification map for Brazil, Meteorol. Z., 22, 711–728, https://doi.org/10.1127/0941-2948/2013/0507, 2013.

Andela, N., Morton, D. C., Giglio, L., Chen, Y., van der Werf, G. R., Kasibhatla, P. S., DeFries, R. S., Collatz, G. J., Hantson, S., Kloster, S., Bachelet, D., Forrest, M., Lasslop, G., Li, F., Mangeon, S., Melton, J. R., Yue, C., and Randerson, J. T.: A human-driven decline in global burned area, Science, 356, 1356–1362, https://doi.org/10.1126/science.aal4108, 2017.

Arpaci, A., Eastaugh, C. S., and Vacik, H.: Selecting the best performing fire weather indices for Austrian ecoregions, Theor. Appl. Climatol., 114, 393–406, https://doi.org/10.1007/s00704-013-0839-7, 2013.

Avitabile, V., Herold, M., Heuvelink, G. B. M., Lewis, S. L., Phillips, O. L., Asner, G. P., Armston, J., Ashton, P. S., Banin, L., Bayol, N., Berry, N. J., Boeckx, P., de Jong, B. H. J., DeVries, B., Girardin, C. A. J., Kearsley, E., Lindsell, J. A., Lopez-Gonzalez, G., Lucas, R., Malhi, Y., Morel, A., Mitchard, E. T. A., Nagy, L., Qie, L., Quinones, M. J., Ryan, C. M., Ferry, S. J. W., Sunderland, T., Laurin, G. V., Gatti, R. C., Valentini, R., Verbeeck, H., Wijaya, A., and Willcock, S.: An integrated pan-tropical biomass map using multiple reference datasets, Global Change Biol., 22, 1406–1420, https://doi.org/10.1111/gcb.13139, 2016.

Beuchle, R., Grecchi, R. C., Shimabukuro, Y. E., Seliger, R., Eva, H. D., Sano, E., and Achard, F.: Land cover changes in the Brazilian Cerrado and Caatinga biomes from 1990 to 2010 based on a systematic remote sensing sampling approach, Appl. Geogr., 58, 116–127, https://doi.org/10.1016/j.apgeog.2015.01.017, 2015.

Bondeau, A., Smith, P. C., Zaehle, S., Schaphoff, S., Lucht, W., Cramer, W., Gerten, D., Lotze-Campen, H., Müller, C., Reichstein, M., and Smith, B.: Modelling the role of agriculture for the 20th century global terrestrial carbon balance, Global Change Biol., 13, 679–706, https://doi.org/10.1111/j.1365-2486.2006.01305.x, 2007.

Chambers, J. Q. and Artaxo, P.: Biosphere–atmosphere interactions: Deforestation size influences rainfall, Nat. Clim. Change, 7, 175, https://doi.org/10.1038/nclimate3238, 2017.

Christian, H. J., Blakeslee, R. J., Boccippio, D. J., Boeck, W. L., Buechler, D. E., Driscoll, K. T., Goodman, S. J., Hall, J. M., Koshak, W. J., Mach, D. M., and Stewart, M. F.: Global frequency and distribution of lightning as observed from space by the Optical Transient Detector, J. Geophys. Res. Atmos., 108, ACL4–1–ACL4–15, https://doi.org/10.1029/2002JD002347, 2003.

Chuvieco, E., Aguado, I., Yebra, M., Nieto, H., Salas, J., Martín, M. P., Vilar, L., Martínez, J., Martín, S., Ibarra, P., de la Riva, J., Baeza, J., Rodríguez, F., Molina, J. R., Herrera, M. A., and Zamora, R.: Development of a framework for fire risk assessment using remote sensing and geographic information system technologies, Ecol. Modell., 221, 46–58, https://doi.org/10.1016/j.ecolmodel.2008.11.017, 2010.

Civil, O. and Environmental Engineering/Princeton University, D.: Global Meteorological Forcing Dataset for Land Surface Modeling, UCAR/NCAR - Research Data Archive, https://rda.ucar.edu/datasets/ds314.0, 2006.

Fader, M., Rost, S., Müller, C., Bondeau, A., and Gerten, D.: Virtual water content of temperate cereals and maize: Present and potential future patterns, J. Hydrol., 384, 218–231, https://doi.org/10.1016/j.jhydrol.2009.12.011, 2010.

Forkel, M., Carvalhais, N., Schaphoff, S., V. Bloh, W., Migliavacca, M., Thurner, M., and Thonicke, K.: Identifying environmental controls on vegetation greenness phenology through model–data integration, Biogeosciences, 11, 7025–7050, https://doi.org/10.5194/bg-11-7025-2014, 2014.

Forkel, M., Dorigo, W., Lasslop, G., Teubner, I., Chuvieco, E., and Thonicke, K.: A data-driven approach to identify controls on global fire activity from satellite and climate observations (SOFIA V1), Geosci. Model Dev., 10, 4443–4476, https://doi.org/10.5194/gmd-10-4443-2017, 2017.

Forkel, M., Andela, N., Harrison, S. P., Lasslop, G., Marle, M. v., Chuvieco, E., Dorigo, W., Forrest, M., Hantson, S., Heil, A., Li, F., Melton, J., Sitch, S., Yue, C., and Arneth, A.: Emergent relationships with respect to burned area in global satellite observations and fire-enabled vegetation models, Biogeosciences, 16, 57–76, https://doi.org/10.5194/bg-16-57-2019, 2019.

Gerten, D., Schaphoff, S., Haberlandt, U., Lucht, W., and Sitch, S.: Terrestrial vegetation and water balance—hydrological evaluation of a dynamic global vegetation model, J. Hydrol., 286, 249–270, https://doi.org/10.1016/j.jhydrol.2003.09.029, 2004.

Giglio, L., Randerson, J. T., and van der Werf, G. R.: Analysis of daily, monthly, and annual burned area using the fourth-generation global fire emissions database (GFED4), J. Geophys. Res. Biogeosci., 118, 317–328, https://doi.org/10.1002/jgrg.20042, 2013.

Goff, J. and Gratch, S.: List 1947, Smithsonian meteorological tables, Transactions of the American Society of Ventilation Engineering, 52, 95, 1946.

Goldewijk, K. K., Beusen, A., van Drecht, G., and de Vos, M.: The HYDE 3.1 spatially explicit database of human-induced global land-use change over the past 12,000 years, Global Ecol. Biogeogr., 20, 73–86, https://doi.org/10.1111/j.1466-8238.2010.00587.x, 2011.

Gupta, H. V., Kling, H., Yilmaz, K. K., and Martinez, G. F.: Decomposition of the mean squared error and NSE performance criteria: Implications for improving hydrological modelling, J. Hydrol., 377, 80–91, https://doi.org/10.1016/j.jhydrol.2009.08.003, 2009.

Hantson, S., Arneth, A., Harrison, S. P., Kelley, D. I., Prentice, I. C., Rabin, S. S., Archibald, S., Mouillot, F., Arnold, S. R., Artaxo, P., Bachelet, D., Ciais, P., Forrest, M., Friedlingstein, P., Hickler, T., Kaplan, J. O., Kloster, S., Knorr, W., Laslop, G., Li, F., Melton, J. R., Meyn, A., Sitch, S., Spessa, A., van der Werf, G. R., Voulgarakis, A., and Yue, C.: The status and challenge of global fire modelling, Copernicus Publications, http://centaur.reading.ac.uk/53498, 2016.

Harvard: Harvard WorldMap, http://worldmap.harvard.edu, [Online; accessed 27. Mar. 2019], 2019.

Hoffmann, W. A., Jackson, R. B., Hoffmann, W. A., and Jackson, R. B.: Vegetation–Climate Feedbacks in the Conversion of Tropical Savanna to Grassland, https://doi.org/10.1175/1520-0442(2000)013<1593:VCFITC>2.0.CO;2, [Online; accessed 28. Mar. 2019], 2000.

IBGE: Mapa de Biomas e de Vegetação, https://ww2.ibge.gov.br/home/presidencia/noticias/21052004biomashtml.shtm, [Online; accessed 14. Feb. 2019], 2019.

Jolly, W. M., Cochrane, M. A., Freeborn, P. H., Holden, Z. A., Brown, T. J., Williamson, G. J., and Bowman, D. M. J. S.: Climate-induced variations in global wildfire danger from 1979 to 2013, Nat. Commun., 6, 7537, https://doi.org/10.1038/ncomms8537, 2015.

Keeley, J. E., Pausas, J. G., Rundel, P. W., Bond, W. J., and Bradstock, R. A.: Fire as an evolutionary pressure shaping plant traits, Trends Plant Sci., 16, 406–411, https://doi.org/10.1016/j.tplants.2011.04.002, 2011.

Keetch, J. J. and Byram, G. M.: A Drought Index for Forest Fire Control, Res. Pap. SE-38. Asheville, NC: U.S. Department of Agriculture, Forest Service, Southeastern Forest Experiment Station. 35 p, 038, https://www.fs.usda.gov/treesearch/pubs/40, 1968.

Kelley, D. I., Prentice, I. C., Harrison, S. P., Wang, H., Simard, M., Fisher, J. B., and Willis, K. O.: A comprehensive benchmarking system for evaluating global vegetation models, Biogeosciences, 10, 3313, https://doi.org/10.5194/bg-10-3313-2013, 2013.

Knorr, W., Arneth, A., and Jiang, L.: Demographic controls of future global fire risk, Nat. Clim. Change, 6, 781, https://doi.org/10.1038/nclimate2999, 2016.

Krawchuk, M. A. and Moritz, M. A.: Constraints on global fire activity vary across a resource gradient, Ecology, 92, 121–132, https://doi.org/10.1890/09-1843.1, 2011.

Lahsen, M., Bustamante, M. M. C., and Dalla-Nora, E. L.: Undervaluing and Overexploiting the Brazilian Cerrado at Our Peril, Environment: Science and Policy for Sustainable Development, 58, 4–15, https://doi.org/10.1080/00139157.2016.1229537, 2016.

Langmann, B., Duncan, B., Textor, C., Trentmann, J., and van der Werf, G. R.: Vegetation fire emissions and their impact on air pollution and climate, Atmos. Environ., 43, 107–116, https://doi.org/10.1016/j.atmosenv.2008.09.047, 2009.

Lasslop, G., Thonicke, K., and Kloster, S.: SPITFIRE within the MPI Earth system model: Model development and evaluation, J. Adv. Model. Earth Syst., 6, 740–755, https://doi.org/10.1002/2013MS000284, 2014.

Lasslop, G., Hantson, S., and Kloster, S.: Influence of wind speed on the global variability of burned fraction: a global fire model's perspective, Int. J. Wildland Fire, 24, 989–1000, https://doi.org/10.1071/WF15052, 2015.

Lasslop, G., Brovkin, V., Reick, C. H., Bathiany, S., and Kloster, S.: Multiple stable states of tree cover in a global land surface model due to a fire-vegetation feedback, Geophys. Res. Lett., 43, 6324–6331, https://doi.org/10.1002/2016GL069365, 2016.

Li, W., MacBean, N., Ciais, P., Defourny, P., Lamarche, C., Bontemps, S., Houghton, R. A., and Peng, S.: Gross and net land cover changes in the main plant functional types derived from the annual ESA CCI land cover maps (1992–2015), Earth Syst. Sci. Data, 10, 219–234, https://doi.org/10.5194/essd-10-219-2018, 2018.

Mebane, Jr., W. R. and Sekhon, J. S.: Genetic Optimization Using Derivatives: The rgenoud Package for R, Journal of Statistical Software, 42, 1–26, https://doi.org/10.18637/jss.v042.i11, 2011.

Moreira de Araújo, F., Ferreira, L. G., and Arantes, A. E.: Distribution Patterns of Burned Areas in the Brazilian Biomes: An Analysis Based on Satellite Data for the 2002–2010 Period, Remote Sens., 4, 1929–1946, https://doi.org/10.3390/rs4071929, 2012.

Nachtergaele, F. O., van Velthuizen, H. T., and Verelst, L.: Harmonized World Soil Database, http://pure.iiasa.ac.at/id/eprint/8958, [Online; accessed 4. Oct. 2018], 2009.

Panisset, J. S., Libonati, R., Gouveia, C. M. P., Machado-Silva, F., França, D. A., França, J. R. A., and Peres, L. F.: Contrasting patterns of the extreme drought episodes of 2005, 2010 and 2015 in the Amazon Basin, Int. J. Climatol., 38, 1096–1104, https://doi.org/10.1002/joc.5224, 2017.

Pechony, O. and Shindell, D. T.: Fire parameterization on a global scale, J. Geophys. Res. Atmos., 114, https://doi.org/10.1029/2009JD011927, 2009.

Prado, D. E.: As caatingas da América do Sul, Ecologia e conservação da Caatinga, 2, 3–74, 2003.

Pyne, S. J., Andrews, P. L., and Laven, R. D.: Introduction to wildland fire, 2nd edition revised, DigitalCommons@USU, https://digitalcommons.usu.edu/barkbeetles/135, 1996.

Quéré, C. L., Moriarty, R., Andrew, R. M., Canadell, J. G., Sitch, S., Korsbakken, J. I., Friedlingstein, P., Peters, G. P., Andres, R. J., Boden, T. A., Houghton, R. A., House, J. I., Keeling, R. F., Tans, P., Arneth, A., Bakker, D. C. E., Barbero, L., Bopp, L., Chang, J., Chevallier, F., Chini, L. P., Ciais, P., Fader, M., Feely, R. A., Gkritzalis, T., Harris, I., Hauck, J., Ilyina, T., Jain, A. K., Kato, E., Kitidis, V., Goldewijk, K. K., Koven, C., Landschützer, P., Lauvset, S. K., Lefèvre, N., Lenton, A., Lima, I. D., Metzl, N., Millero, F., Munro, D. R., Murata, A., Nabel, J. E. M. S., Nakaoka, S., Nojiri, Y., O'Brien, K., Olsen, A., Ono, T., Pérez, F. F., Pfeil, B., Pierrot, D., Poulter, B., Rehder, G., Rödenbeck, C., Saito, S., Schuster, U., Schwinger, J., Séférian, R., Steinhoff, T., Stocker, B. D., Sutton, A. J., Takahashi, T., Tilbrook, B., van der Laan-Luijkx, I. T., van der Werf, G. R., van Heuven, S., Vandemark, D., Viovy, N., Wiltshire, A., Zaehle, S., and Zeng, N.: Global Carbon Budget 2015, Earth Syst. Sci. Data, 7, 349–396, https://doi.org/10.5194/essd-7-349-2015, 2015.

Rabin, S. S., Ward, D. S., Malyshev, S. L., Magi, B. I., Shevliakova, E., and Pacala, S. W.: A fire model with distinct crop, pasture, and non-agricultural burning: use of new data and a model-fitting algorithm for FINAL.1, Geosci. Model Dev., 11, 815–842, https://doi.org/10.5194/gmd-11-815-2018, 2018.

Ray, D., Nepstad, D., and Moutinho, P.: MICROMETEOROLOGICAL AND CANOPY CONTROLS OF FIRE SUSCEPTIBILITY IN A FORESTED AMAZON LANDSCAPE, Ecol. Appl., 15, 1664–1678, https://doi.org/10.1890/05-0404, 2005.

Rodell, M., Houser, P. R., Jambor, U., Gottschalck, J., Mitchell, K., Meng, C.-J., Arsenault, K., Cosgrove, B., Radakovich, J., Bosilovich, M., Entin, J. K., Walker, J. P., Lohmann, D., Toll, D., Rodell, M., Houser, P. R., Jambor, U., Gottschalck, J., Mitchell, K., Meng, C.-J.,

Arsenault, K., Cosgrove, B., Radakovich, J., Bosilovich, M., Entin, J. K., Walker, J. P., Lohmann, D., and Toll, D.: The Global Land Data Assimilation System, Bull. Am. Meteorol. Soc., https://doi.org/10.1175/BAMS-85-3-381, 2004.

Rogers, B. M., Soja, A. J., Goulden, M. L., and Randerson, J. T.: Influence of tree species on continental differences in boreal fires and climate feedbacks, Nat. Geosci., 8, 228, https://doi.org/10.1038/ngeo2352, 2015.

Roitman, I., Bustamante, M. M. C., Haidar, R. F., Shimbo, J. Z., Abdala, G. C., Eiten, G., Fagg, C. W., Felfili, M. C., Felfili, J. M., Jacobson, T. K. B., Lindoso, G. S., Keller, M., Lenza, E., Miranda, S. C., Pinto, J. R. R., Rodrigues, A. A., Delitti, W. B. C., Roitman, P., and Sampaio, J. M.: Optimizing biomass estimates of savanna woodland at different spatial scales in the Brazilian Cerrado: Re-evaluating allometric equations and environmental influences, PLoS One, 13, e0196 742, https://doi.org/10.1371/journal.pone.0196742, 2018.

Rothermel, R. C.: A mathematical model for predicting fire spread in wildland fuels, DigitalCommons@USU, Res. Pap. INT-115, 1, https://digitalcommons.usu.edu/barkbeetles/438, 1972.

Schaphoff, S., Heyder, U., Ostberg, S., Gerten, D., Heinke, J., and Lucht, W.: Contribution of permafrost soils to the global carbon budget, Environ. Res. Lett., 8, 014 026, https://doi.org/10.1088/1748-9326/8/1/014026, 2013.

Schaphoff, S., Bloh, W. v., Rammig, A., Thonicke, K., Biemans, H., Forkel, M., Gerten, D., Heinke, J., Jägermeyr, J., Knauer, J., Langerwisch, F., Lucht, W., Müller, C., Rolinski, S., and Waha, K.: LPJmL4 – a dynamic global vegetation model with managed land – Part 1: Model description, Geosci. Model Dev., 11, 1343–1375, https://doi.org/10.5194/gmd-11-1343-2018, 2018a.

Schaphoff, S., Forkel, M., Müller, C., Knauer, J., Bloh, W. v., Gerten, D., Jägermeyr, J., Lucht, W., Rammig, A., Thonicke, K., and Waha, K.: LPJmL4 – a dynamic global vegetation model with managed land – Part 2: Model evaluation, Geosci. Model Dev., 11, 1377–1403, https://doi.org/10.5194/gmd-11-1377-2018, 2018b.

Seager, R., Hooks, A., Williams, A. P., Cook, B., Nakamura, J., Henderson, N., Seager, R., Hooks, A., Williams, A. P., Cook, B., Nakamura, J., and Henderson, N.: Climatology, Variability, and Trends in the U.S. Vapor Pressure Deficit, an Important Fire-Related Meteorological Quantity∗, https://journals.ametsoc.org/doi/abs/10.1175/JAMC-D-14-0321.1, [Online; accessed 19. Oct. 2018], 2015.

Sedano, F. and Randerson, J.: Multi-scale influence of vapor pressure deficit on fire ignition and spread in boreal forest ecosystems, https://doi.org/10.5194/bg-11-3739-2014, [Online; accessed 11. Oct. 2018], 2014.

Silvério, D. V., Brando, P. M., Balch, J. K., Putz, F. E., Nepstad, D. C., Oliveira-Santos, C., and Bustamante, M. M. C.: Testing the Amazon savannization hypothesis: fire effects on invasion of a neotropical forest by native cerrado and exotic pasture grasses, Philosophical Transactions of the Royal Society B: Biological Sciences, https://royalsocietypublishing.org/doi/full/10.1098/rstb.2012.0427, 2013.

Sitch, S., Smith, B., Prentice, I. C., Arneth, A., Bondeau, A., Cramer, W., Kaplan, J. O., Levis, S., Lucht, W., Sykes, M. T., Thonicke, K., and Venevsky, S.: Evaluation of ecosystem dynamics, plant geography and terrestrial carbon cycling in the LPJ dynamic global vegetation model, Global Change Biol., 9, 161–185, https://doi.org/10.1046/j.1365-2486.2003.00569.x, 2003.

Thonicke, K., Venevsky, S., Sitch, S., and Cramer, W.: The role of fire disturbance for global vegetation dynamics: coupling fire into a Dynamic Global Vegetation Model, Global Ecol. Biogeogr., 10, 661–677, https://doi.org/10.1046/j.1466-822X.2001.00175.x, 2001.

Thonicke, K., Spessa, A., Prentice, I. C., Harrison, S. P., Dong, L., and Carmona-Moreno, C.: The influence of vegetation, fire spread and fire behaviour on biomass burning and trace gas emissions: results from a process-based model, Biogeosciences, 7, 1991–2011, https://doi.org/10.5194/bg-7-1991-2010, 2010.

van der Werf, G. R., Dempewolf, J., Trigg, S. N., Randerson, J. T., Kasibhatla, P. S., Giglio, L., Murdiyarso, D., Peters, W., Morton, D. C., Collatz, G. J., Dolman, A. J., and DeFries, R. S.: Climate regulation of fire emissions and deforestation in equatorial Asia, Proc. Natl. Acad. Sci. U.S.A., 105, 20 350–20 355, https://doi.org/10.1073/pnas.0803375105, 2008.

Venevsky, S., Thonicke, K., Sitch, S., and Cramer, W.: Simulating fire regimes in human-dominated ecosystems: Iberian Peninsula case study, Global Change Biol., 8, 984–998, https://doi.org/10.1046/j.1365-2486.2002.00528.x, 2002.

Wagner, C. E. V., Forest, P., Station, E., Ontario, C. R., Francais, R. U. E., and Davis, H. J.: Development and Structure of the Canadian Forest FireWeather Index System, Can. For. Serv., Forestry Tech. Rep, 1987.

Werf, G. R. v. d., Randerson, J. T., Giglio, L., Collatz, G. J., Mu, M., Kasibhatla, P. S., Morton, D. C., DeFries, R. S., Jin, Y., and Leeuwen, T. T. v.: Global fire emissions and the contribution of deforestation, savanna, forest, agricultural, and peat fires (1997–2009), Atmos. Chem. Phys., 10, 11 707–11 735, https://doi.org/10.5194/acp-10-11707-2010, 2010.

Werf, G. R. v. d., Randerson, J. T., Giglio, L., Leeuwen, T. T. v., Chen, Y., Rogers, B. M., Mu, M., Marle, M. J. E. v., Morton, D. C., Collatz, G. J., Yokelson, R. J., and Kasibhatla, P. S.: Global fire emissions estimates during 1997–2016, Earth Syst. Sci. Data, 9, 697–720, https://doi.org/10.5194/essd-9-697-2017, 2017.

Willmott, C. J. and Willmott, C. J.: Some Comments on the Evaluation of Model Performance, Bull. Am. Meteorol. Soc., https://doi.org/10.1175/1520-0477(1982)063<1309:SCOTEO>2.0.CO;2, 1982.

Wilson, R. A.: A reexamination of fire spread in free-burning porous fuel beds /, http://www.sidalc.net/cgi-bin/wxis.exe/?IsisScript=COLPOS.xis&method\=post&formato=2&cantidad=1&expresion=mfn=001388, [Online; accessed 4. Oct. 2018], 1982.

Yue, X. and Unger, N.: Fire air pollution reduces global terrestrial productivity, Nat. Commun., 9, 5413, https://doi.org/10.1038/s41467-018-07921-4, 2018.